

# Synthesis and Characterization of Polycyanurate Networks Modified by Oligo( $\epsilon$ -caprolactone) as Precursors of Porous Thermosets

A. Fainleib,<sup>1</sup> O. Grigoryeva,<sup>1</sup> M. R. Garda,<sup>2</sup> J. M. Saiter,<sup>2</sup> F. Lauprêtre,<sup>3</sup> C. Lorthioir,<sup>3</sup> D. Grande<sup>3</sup>

<sup>1</sup>Institute of Macromolecular Chemistry, National Academy of Sciences of Ukraine, 02160 Kyiv, Ukraine

<sup>2</sup>Laboratoire Polymères-Biopolymères-Membranes, UMR 6522 CNRS - Université de Rouen, site du Madrillet, avenue de l'Université, BP 12, 76801 Saint Etienne du Rouvray, France

<sup>3</sup>Equipe « Systèmes Polymères Complexes », Institut de Chimie et des Matériaux Paris-Est, UMR 7182 CNRS - Université Paris XII - Val-de-Marne, 2, rue Henri Dunant, 94320 Thiais, France

Received 22 February 2007; accepted 9 June 2007

DOI 10.1002/app.27039

Published online 4 September 2007 in Wiley InterScience (www.interscience.wiley.com).

**ABSTRACT:** Oligo( $\epsilon$ -caprolactone)-modified polycyanurate networks were synthesized by thermal polycyclotrimerization of dicyanate ester of bisphenol E in the presence of a dihydroxy-telechelic poly( $\epsilon$ -caprolactone) (PCL) oligomer with varying compositions. Using FTIR, gel fraction content and density measurements, it has been proved that the main part of the reactive modifier was chemically incorporated into the PCN network structure. According to the thermal behavior of the polymer networks as investigated by TGA, they can be divided into two groups. The first group of systems with low modifier content (i.e., up to 20 wt %) is characterized by one stage of decomposition under nitrogen, and

two stages under oxygen. A second group of systems with higher modifier content is generally characterized by two stages of decomposition in nitrogen and three stages in oxygen. DSC and DMTA investigations have shown the occurrence of at least a two-phase structure in all the samples. The PCN/PCL-based hybrid networks can be effectively used as precursors for the generation of porous PCN thermosets, as evidenced by FTIR and SEM. © 2007 Wiley Periodicals, Inc. *J Appl Polym Sci* 106: 3929–3938, 2007

**Key words:** polycyanurate networks; oligo( $\epsilon$ -caprolactone); thermal behavior; phase structure; porous thermosets

## INTRODUCTION

Polycyanurate (PCN) networks offer a combination of excellent thermal and dimensional stability, which make them suitable for their use in high performance technology (e.g., as matrices for composites in high-speed electronic circuitry and transportation). For the electronics market, the attractive features of PCNs are their low dielectric constants (2.6–3.2), high glass transition temperatures ( $T_g \sim 220$ – $270^\circ\text{C}$ ), high purity, inherent flame-retardancy (giving the potential to eliminate brominated flame retardants), and high adhesion to conductor metals at temperatures higher than  $250^\circ\text{C}$ .<sup>1</sup> Several reviews collecting the numerous investigations in the field of PCN synthesis, processing, characterization, modification, and applications have appeared since the early 1990s.<sup>1–7</sup> Recently, we have published several papers dealing

with the modification of PCNs by dihydroxy-telechelic polyethers or polyesters.<sup>8–11</sup> It was found that the modifiers were partly chemically incorporated into the PCN structure through the reaction of their terminal hydroxyl groups with cyanate groups of growing PCN network.

In contrast, few reports on the design and synthesis of porous PCNs have been published.<sup>12–14</sup> Interest in closed cell porous structures arises from the possibility to significantly lower the intrinsic dielectric constant. Kiefer et al.<sup>12,13</sup> synthesized such porous systems from dicyanate of bisphenol E (DCBE) using cyclohexane as a porogen. The strategy employed was based on the generation of a two-phase morphology, where the dispersed phase mainly consists of a nonreactive low molar mass liquid having a low boiling point. The generation of the foam structure was accomplished by removing the porogen upon heating. The porosity of the resulting materials was estimated using density measurements, determination of dielectric constants, and scanning electron microscopy (SEM). Hedrick et al.<sup>14</sup> synthesized PCN systems containing thermally labile segments, which led to the formation of porous networks upon thermolysis, and after removing the destruction products from the resulting materials. In such investigation, the PCN systems were synthe-

Correspondence to: A. Fainleib (fainleib@i.kiev.ua).

Contract grant sponsor: National Academy of Sciences of Ukraine (NASU); contract grant number: 16813.

Contract grant sponsor: Centre National de la Recherche Scientifique (CNRS), Ukraine-France cooperation; contract grant number: 18973.

*Journal of Applied Polymer Science*, Vol. 106, 3929–3938 (2007)  
© 2007 Wiley Periodicals, Inc.

sized from 4,4'-(hexafluoroisopropylidene)diphenylcyanate in the presence of either poly(propylene oxide) or a propylene oxide-urethane copolymer as the thermally unstable component. The propylene oxide-based oligomers were miscible with the cyanate monomer over the entire range of compositions studied, but developed a two-phase structure upon reaction to form a thermoplastic-modified PCN thermoset. Upon thermal decomposition of the propylene oxide segments, however, the foam was found to collapse. The pore collapse might be related to an increase of polymer chain mobility in the PCN network at temperatures close to  $T_g$ .

The scarcity of studies on the manufacture of porous PCN thermosets with controlled porosity has prompted us to develop an alternative approach for the generation of porous PCN networks without using high temperatures. The main idea relies on the synthesis of PCNs containing hydrolyzable fragments, followed by their selective removal upon mild hydrolysis. In this first contribution, we essentially describe the synthesis and characterization of PCN systems from DCBE and a dihydroxy-telechelic oligomer of poly( $\epsilon$ -caprolactone) (PCL) to establish clear correlations between their structure and their properties. The investigation of the structure-property relationships in these PCL-modified PCN networks holds relevance for a better understanding of their further utilization as precursors of porous thermosets.

The present article focuses on the preparation of novel PCN/PCL-based hybrid networks and their characterization by different physicochemical techniques, namely FTIR, pycnometry, thermogravimetric analysis (TGA), differential scanning calorimetry (DSC), and dynamic mechanical thermal analysis (DMTA). The possibility of producing porous PCN thermosets by basic hydrolysis of PCL fragments of the modified PCN networks is also addressed. The preliminary results given by FTIR and SEM analyses of the hydrolyzed PCN/PCL systems are presented.

## EXPERIMENTAL

### Materials and sample preparation

1,1'-bis(4-cyanatophenyl)ethane (dicyanate ester of bisphenol E, DCBE) under the trade name ARO Cy L-10, was kindly supplied by Huntsman (Huntsman Advanced Materials, NY) and was used as received. Dihydroxy-telechelic PCL ( $M_n = 2000 \text{ g mol}^{-1}$ ,  $M_w/M_n = 2.1$ ) was purchased from Aldrich (Sigma-Aldrich Biotechnology, ALSI, Kiev, Ukraine) and used as received. PCL was dissolved in the melt of DCBE at  $100^\circ\text{C}$  and degassed for 5 min at the same temperature under vacuum. The PCN(DCBE)/PCL mass compositions used were equal to 100/0, 95/5, 90/10,

85/15, 80/20, 70/30, 60/40, 50/50, and 0/100 wt %, respectively. The systems prepared were poured into a PTFE-coated mold. The curing cycle consisted of three stages: 5 h at  $150^\circ\text{C}$ , then 3 h at  $180^\circ\text{C}$ , and finally 1 h at  $210^\circ\text{C}$ .

### Gel fraction determination

To evaluate the incorporation degree of PCL into the PCN network for samples produced, the residual gel content was determined via Soxhlet extraction using acetone. The extraction was carried out for 16 h, and then the insoluble fractions were dried in an oven (at  $50^\circ\text{C}$  for 24 h) prior to weighing. The experimental values of gel fractions ( $w_{g \text{ exp}}$ ) were defined as the mass percentages of the insoluble parts of the PCN/PCL systems. The theoretical values of gel fractions ( $w_{g \text{ theor}}$ ) were calculated using eq. (1),<sup>15</sup> with conjecture that linear PCL was completely extracted:

$$w_{g \text{ theor}} = (100 - w_{\text{PCL}}) \times (2\alpha - 1)/\alpha^2 \quad (1)$$

where  $w_{\text{PCL}}$  is the mass fraction of PCL in the initial compositions and  $\alpha$  is the OCN-conversion calculated from FTIR data using the intensity of the characteristic absorbance of the  $\text{C}\equiv\text{N}$  triple bond at  $2236\text{--}2272 \text{ cm}^{-1}$ . The height of the peak at  $2968 \text{ cm}^{-1}$  corresponding to  $\text{CH}_3$  group was used as an internal standard.

Therefore, the OCN-conversion ( $\alpha$ ) was calculated using eq. (2) as follows:

$$\alpha = 1 - \frac{A_{2236-2272}^{\text{PCN}}}{A_{2236-2272}^{\text{DCBE}}} \quad (2)$$

where  $A_{2236-2272}^{\text{PCN}}$  and  $A_{2236-2272}^{\text{DCBE}}$  are the absorbance values of the integrated bands from  $2236$  to  $2272 \text{ cm}^{-1}$  associated with the stretching vibration of cyanate ( $\text{OC}\equiv\text{N}$ ) groups in PCN and DCBE, respectively.

### Generation of porous thermosetting materials

The PCN/PCL-based thin films were placed in a 1 : 1 mixture of phosphate buffer solution (pH = 8.16)/ethanol, and maintained for 250 h at  $70^\circ\text{C}$ . After hydrolysis, the samples were washed with distilled water up to neutral pH and dried at  $60^\circ\text{C}$  under vacuum up to constant weight.

### Physicochemical techniques

#### FTIR spectroscopy

FTIR spectra were recorded on a Bruker model Tensor 27 DTGS spectrometer between  $4000$  and

450  $\text{cm}^{-1}$  using the Attenuated Total Reflection (ATR) mode. For each spectrum, 32 consecutive scans with a resolution of 4  $\text{cm}^{-1}$  were averaged. The degree of OCN-conversion was calculated from the intensity of the OCN stretching absorption band at 2272  $\text{cm}^{-1}$ .

#### Density measurements

The density ( $\rho$ , average value over five measurements) of the samples was determined using Archimedes's balance method at temperature  $T = (20 \pm 1)^\circ\text{C}$ . The theoretical values of density ( $\rho_{\text{theor}}$ ) were calculated from the following additive law [eq. (3)]:

$$\rho_{\text{theor}} = \phi_1\rho_1 + \phi_2\rho_2 \quad (3)$$

where  $\phi_1$ ,  $\phi_2$  are the volume fractions and  $\rho_1$ ,  $\rho_2$  refers to the densities of PCN and PCL, respectively. The volume fractions were calculated taking into account the mass fractions and the density values of both components.

#### Thermogravimetric analysis

Thermogravimetry measurements were performed on a Netzsch TG 209 thermobalance under inert atmosphere (nitrogen flow of 1.5 mL/min) and under oxydative atmosphere (oxygene flow of 1.5 mL/min). Sample pellets, with masses ranging from 10 to 20 mg, were put in aluminum oxide crucibles, and then heated at  $10^\circ\text{C}/\text{min}$  from  $30^\circ\text{C}$  up to  $900^\circ\text{C}$ .

#### Differential scanning calorimetry

DSC measurements were carried out with a TA Instruments Q100 calorimeter under a nitrogen atmosphere. Samples were first heated from 40 to  $300^\circ\text{C}$  with a scan rate of  $20^\circ\text{C}/\text{min}$ , and subsequently cooled to  $-100^\circ\text{C}$ . A second scan was performed under the same heating conditions. The  $T_g$  values were measured in the second run: to determine a  $T_g$  range, the lower ( $T_{g \text{ onset}}$ ) and upper ( $T_{g \text{ end}}$ ) limits were identified as the values associated with the intercepts of tangent to midpoint of the specific heat increment with "glassy" and "viscous" base-lines, respectively.

#### Dynamic mechanical thermal analysis

DMTA was carried out with a TA Instruments Q800 thermal analyzer in tension mode. Rectangular samples were cut from films within the following range of dimensions: length of 10 mm, width of 10 mm, and thickness of 0.08 mm. Storage modulus ( $E'$ ), loss modulus ( $E''$ ) and loss factor ( $\tan \delta$ ) were measured

between  $-100$  and  $300^\circ\text{C}$  at a heating rate of  $3^\circ\text{C}/\text{min}$  and a frequency of 1 Hz. Samples were stretched by an initial stress of 0.04 N; the strain amplitude was set to 0.1% and measurements were performed over four cycles of deformation.

#### Scanning electron microscopy

SEM micrographs were obtained using a LEO 1530 microscope equipped with a high-vacuum ( $10^{-10}$  mmHg) Gemini Column. The accelerating tensions ranged from 1 to 5 kV, two detectors (InLens and Secondary Electron) were used. Prior to analyses, the polymer films were cryofractured and coated with a Pd/Au alloy (4 nm of thickness) in a Cressington 208 HR sputter-coater.

## RESULTS AND DISCUSSION

A reaction scheme associated with the polycyclotrimerization of pure dicyanate monomer (DCBE) leading to the formation of a PCN network is shown in Figure 1. FTIR spectra of the neat PCN network, the PCL oligomeric modifier and a typical cured PCN/PCL system are presented in Figure 2. In the spectra of neat PCN and PCN/PCL networks, the absence of the bands with maxima at  $2236\text{--}2272 \text{ cm}^{-1}$  associated with the stretching vibration of cyanate ( $\text{OC}\equiv\text{N}$ ) groups denotes the completion of reactions involved in PCN formation.<sup>1</sup> Moreover, no unreacted  $\text{OC}\equiv\text{N}$  groups were detected in FTIR spectra of the sol fractions of the latter samples (after acetone

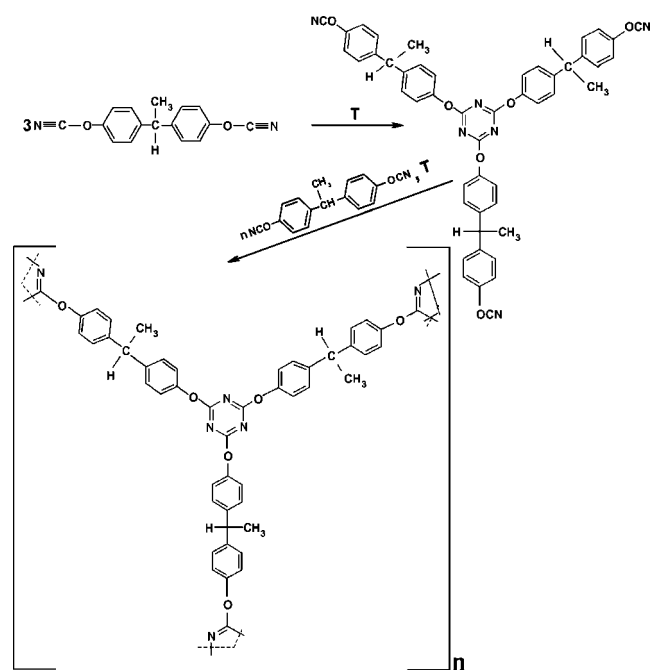


**Figure 1** Polycyclotrimerization of DCBE cyanate monomer.

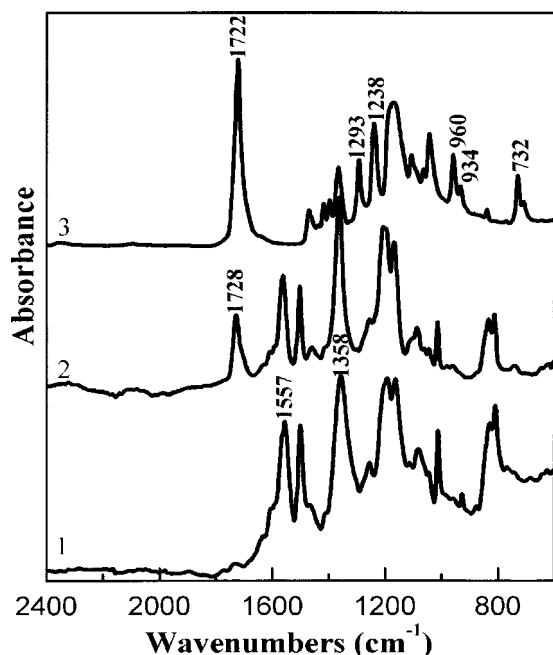


**Figure 2** FTIR spectra for (1) the neat PCN network, (2) the PCN/PCL system with a 50/50 wt % composition, and (3) PCL oligomer.

extraction), thus indicating that DCBE was completely integrated into the PCN network structure. On the other hand, one can see the appearance of strong absorption bands at 1358 and 1557  $\text{cm}^{-1}$  arising from the stretching vibrations of the cyanurate rings (triazine and phenyl-oxygen-triazine bands, respectively).<sup>1</sup>

The carbonyl ( $\text{C}=\text{O}$ ) absorption band at 1728  $\text{cm}^{-1}$  was observed in all FTIR spectra of PCN/PCL systems studied, thus confirming the presence of PCL subchains. The absence of the bands at 1293  $\text{cm}^{-1}$  ( $\text{C}-\text{O}$  and  $\text{C}-\text{C}$  stretching vibrations), 1238 and 934  $\text{cm}^{-1}$  (asymmetric  $\text{C}-\text{O}-\text{C}$  and symmetric  $\text{C}-\text{O}-\text{C}$  stretching vibrations, respectively), as well as those at 960, 732, and 709  $\text{cm}^{-1}$  (in-phase rock vibrations of  $\text{CH}_2$  groups) corresponding to crystalline phase<sup>16,17</sup> gives evidence that the PCL segments do not crystallize in the PCN matrix. Figure 3 shows the process of chemical incorporation of a dihydroxy-telechelic polyester into the PCN structure, as it was recently proposed by Fainleib et al.<sup>8-11</sup> Because of the fast decomposition of the intermediate product, namely the iminocarbonate (IC), it was not possible to observe a specific band of the product resulting from the reaction of terminal alcohol functions of PCL with cyanate groups of PCN.

The specific character of the subsequent reaction of the IC into triazine ring lies in the possibility of exchange of hydroxyl and cyanate groups between the reacting units.<sup>1</sup> Grigat and Putter<sup>18</sup> observed that the most acidic phenol was released, and thus, a

substituted triazine ring should be obtained with the liberation of a monophenol deriving from DCBE (MCBE). In the case of such an exchange, the oligomeric dicyanate (ODC) derived from PCL has to be obtained simultaneously. Thus, three kinds of cyanate molecules, i.e., DCBE, monocyanate ester of bisphenol E (MCBE) and ODC (formed from IC) participate in the PCN network formation.

The extent of PCL chemical incorporation into PCN structures was established by comparison between experimental and calculated values of gel fraction contents (see Experimental). As shown in Table I, regardless of the PCN/PCL composition, the experimental value of gel fraction was higher than that calculated. Moreover, the higher the PCL content in the initial composition, the greater the difference between experimental and theoretical values. These results clearly reveal that a significant part of PCL was covalently linked to the PCN network structure and could not be extracted from the system. According to the calculated data presented in Table I, conversions higher than 50 wt % were associated with the amounts of PCL that were chemically incorporated into the network structure. Therefore, a residual part of PCL was unreacted and could not be incorporated into the PCN structure. FTIR analyses of sol fractions confirmed that they were constituted of PCL oligomers. Furthermore, it is noteworthy that all networks were transparent before and

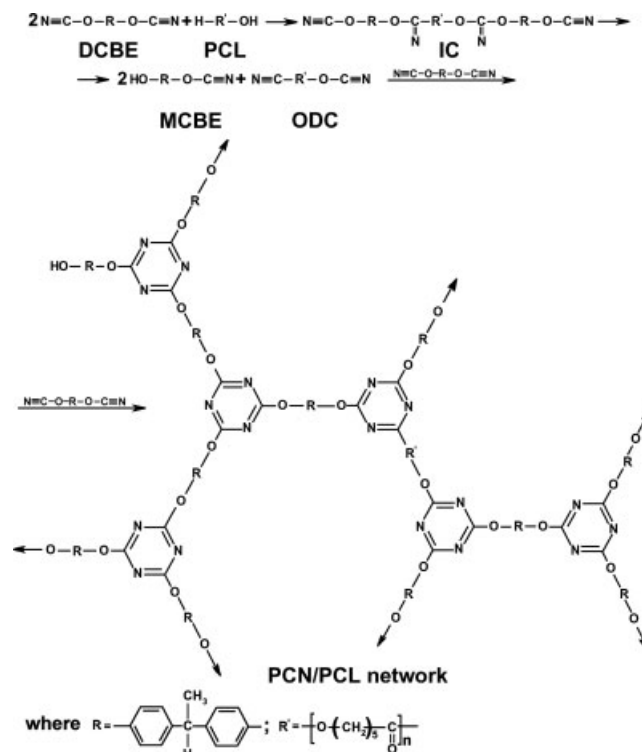


**Figure 3** Reaction scheme associated with chemical incorporation of dihydroxy-telechelic PCL into PCN structure.

TABLE I  
Gel Fractions of Cured PCN/PCL Systems as a Function of Composition

| PCL content in initial composition (wt %), $w_{\text{PCL}}$ | Gel fraction content (wt %), $w_g$ |                       | PCL incorporation degree (wt %), $\Delta w_g^a/w_{g \text{ exp}} 100$ | PCL conversion at incorporation (wt %), $\Delta w_g^a/w_{\text{PCL}} 100$ |
|---|------------------------------------|-----------------------|---|---|
|   | $w_{g \text{ exp}}$                | $w_{g \text{ theor}}$ |   |   |
| 0   | 98.7                               | 98.7                  | 0   | 0   |
| 5   | 97.9                               | 93.8                  | 4   | 82  |
| 10  | 94.9                               | 88.8                  | 6   | 61  |
| 15  | 94.3                               | 83.9                  | 11  | 69  |
| 20  | 92.1                               | 79.0                  | 14  | 66  |
| 30  | 83.8                               | 69.1                  | 18  | 49  |
| 40  | 82.1                               | 59.2                  | 28  | 57  |
| 50  | 77.7                               | 49.4                  | 36  | 57  |

$$^a \Delta w_g = w_{g \text{ exp}} - w_{g \text{ theor}}$$

after extraction, suggesting a good degree of miscibility between PCL subchains and PCN network. Considering that the difference between the refractive indices of both components is significant ( $n_D^{25}$  (PCL) = 1.49 and  $n_D^{25}$  (PCN) = 1.53), the transparency of samples is at least indicative of the occurrence of microdomains smaller than the visible wavenumbers, i.e., about a few hundreds of nanometers.

The experimental and calculated (using additive law) values of density for the samples under study are reported in Figure 4. It appears that up to 10 wt % of PCL, the additive law seems to be respected, whereas a positive deviation is observed for compositions with a higher content of PCL. This positive deviation from the additive law is consistent with the occurrence of chemical embedding of PCL modifier into the PCN network.<sup>19</sup> One can see that the higher the content of PCL incorporated into PCN (cf.

Table I), the more significant the deviation between experimental and additive values of density.

Table II and Figure 5 display the data of TGA for PCN/PCL systems. Obviously enough, all the systems investigated could be considered as thermally stable polymers. The differences between the results obtained under nitrogen and those under oxygen were evident. It should be noted that the systems with a PCL content lower than or equal to 20 wt % were characterized by quite high char residues (20–45 wt % depending on composition) under nitrogen. There was also an obvious composition dependence of thermal behavior of PCN/PCL systems. The compositions with low content of PCL, i.e., up to 20 wt %, were characterized by one stage of decomposition in nitrogen, and two stages under oxygen, because of thermal oxidative destruction. The onset temperature of intensive decomposition ( $T_{d \text{ onset}}$ ) in oxygen for these compositions was higher than 375°C. A second group of compositions, namely those with a PCL content higher than or equal to 30 wt %, was generally characterized by two stages of decomposition in nitrogen and three stages in oxygen (thermal oxidative destruction). We suppose that the thermal behavior for the first group of compositions mainly arose from the single contribution of the PCN network chemically modified by PCL segments. Nevertheless, for the second group of compositions, the contribution of unreacted free PCL to thermal properties of the network systems became more significant. Even though the thermal stability of the networks was certainly higher under nitrogen than under oxygen, it can be concluded that all PCN/PCL systems exhibited quite similar thermal stability at temperatures lower than 400°C in both atmospheres. Such a thermal feature is very important for their further practical application.

Figure 6 shows the DSC traces for neat PCN, pure PCL, and several PCN/PCL systems. We can observe the endothermic peak corresponding to the

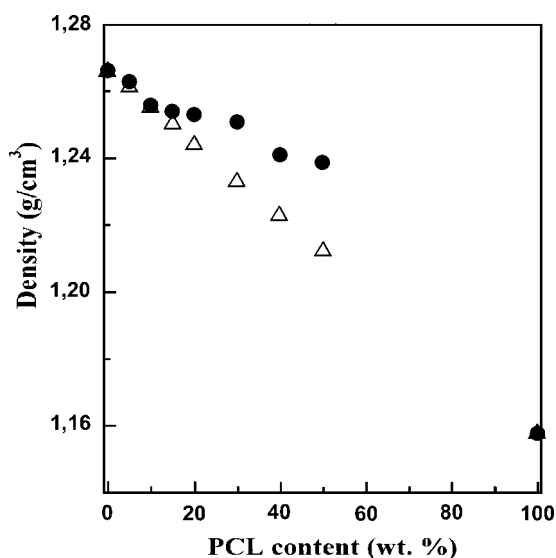


Figure 4 Composition dependence of (●) experimental and (△) additive values of density for PCN/PCL systems.

TABLE II  
Thermal Properties of PCN/PCL Systems as Investigated by TGA

| PCN/PCL<br>composition<br>(wt %) | Thermal decomposition (under N <sub>2</sub> ) |                    |                   |                    |                 |                           | Thermal-oxidative decomposition (under O <sub>2</sub> ) |                    |                   |                    |                 |                    |                 |                           |
|----------------------------------|---|--------------------|-------------------|--------------------|-----------------|---------------------------|---|--------------------|-------------------|--------------------|-----------------|--------------------|-----------------|---------------------------|
|                                  | $T_{d\ 5\%}^a$<br>(°C)                        | $T_{d1}^b$<br>(°C) | $m_1^c$<br>(wt %) | $T_{d2}^b$<br>(°C) | $m_2$<br>(wt %) | Char<br>residue<br>(wt %) | $T_{d\ 5\%}^a$<br>(°C)                                  | $T_{d1}^b$<br>(°C) | $m_1^c$<br>(wt %) | $T_{d2}^b$<br>(°C) | $m_2$<br>(wt %) | $T_{d3}^b$<br>(°C) | $m_3$<br>(wt %) | Char<br>residue<br>(wt %) |
| 100/0                            | 411   | –                  | –                 | 427                | 17              | 46                        | 406   | –                  | –                 | 420                | 19              | 540                | 69              | 0.2                       |
| 95/5                             | 401   | –                  | –                 | 423                | 23              | 39                        | 400   | –                  | –                 | 417                | 24              | 533                | 71              | 0.6                       |
| 90/10                            | 391   | –                  | –                 | 421                | 28              | 35                        | 388   | –                  | –                 | 413                | 28              | 533                | 75              | 0.3                       |
| 85/15                            | 384   | –                  | –                 | 419                | 30              | 33                        | 380   | –                  | –                 | 412                | 31              | 529                | 76              | 0.4                       |
| 80/20                            | 348   | –                  | –                 | 415                | 35              | 30                        | 331   | –                  | –                 | 407                | 35              | 527                | 78              | 0.2                       |
| 70/30                            | 268   | 299                | 10                | 409                | 48              | 20                        | 253   | 328                | 17                | 383                | 47              | 518                | 87              | 0.1                       |
| 60/40                            | 256   | 288                | 12                | 393                | 49              | 2                         | 249   | 328                | 19                | 383                | 37              | 508                | 83              | 0.1                       |
| 50/50                            | 255   | 291                | 11                | 396                | 51              | 3                         | 246   | 331                | 30                | –                  | –               | 513                | 80              | 0.1                       |
| 0/100                            | 280   | 284                | 6                 | 393                | 67              | 2                         | 220   | 275                | 56                | 327                | 91              | 461                | 98              | 0.3                       |

<sup>a</sup>  $T_{d\ 5\%}$ : degradation temperature identified as the temperature value at 5% of mass loss.

<sup>b</sup>  $T_{di}$ : temperature value of maximum rate of degradation at the degradation Stage  $i$  considered.

<sup>c</sup>  $m_i$ : mass loss value at degradation temperature  $T_{di}$ .

melting of pure PCL around 50°C, and this peak does not appear in the DSC curves associated with PCN/PCL systems, even at the highest PCL content (50 wt %) considered. This confirms the conclusion drawn from FTIR measurements, noting that PCL does not crystallize within the PCN network for all the compositions studied. Moreover, it can be seen that single glass transitions were observed for PCL contents ranging from 5 to 50 wt %. A summary of the corresponding glass transition ranges—the onset temperature ( $T_{g\ onset}$ ) and the final one ( $T_{g\ end}$ ) in particular—is reported in Table III. Clearly, both  $T_{g\ onset}$  and  $T_{g\ end}$  were shifted toward lower values with increasing the PCL content. This variation results from the insertion of soft PCL subchains into

the PCN network: as in the case of the single phase-state of miscible polymer blends, the increase of the mass fraction related to the low- $T_g$  component induced a decrease in the glass transition temperature. In addition, the occurrence of nonincorporated PCL oligomer in the PCN/PCL systems considered in this study may certainly play a role in the composition dependence of the calorimetric  $T_g$ : the oligo( $\epsilon$ -caprolactone) should act as a plasticizer and the corresponding effect should be more pronounced with increasing the percentage of free PCL subchains, so in turn the PCL content (see Table I).

The composition dependence of the  $T_g$  values for PCN/PCL systems did not match those calculated from the Fox equation for miscible polymer blends:

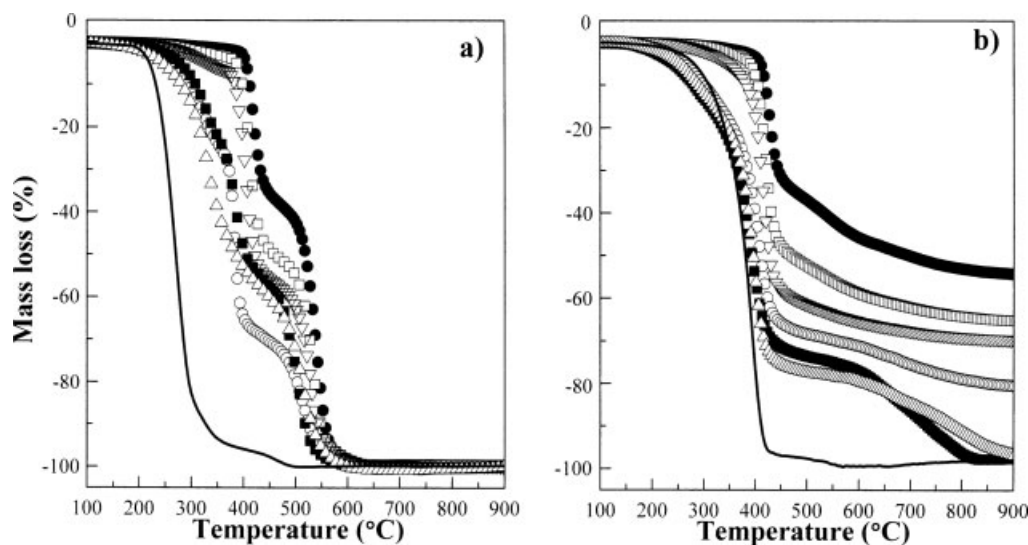
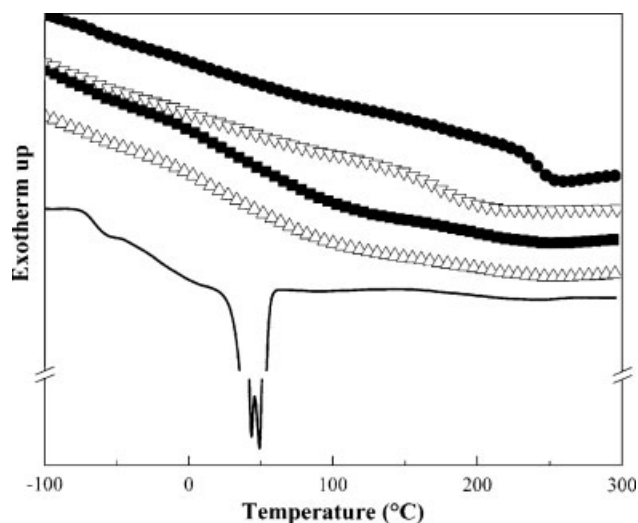


Figure 5 Mass loss curves from TGA for PCN/PCL systems with different compositions (wt %): (●) pure PCN; (□) 90/10; (▽) 80/20; (○) 70/30; (■) 60/40; (△) 50/50; and (—) pure PCL. Analyses in oxygen (a) and in nitrogen atmosphere (b).



**Figure 6** Typical DSC thermograms (second heating scan) for several PCN/PCL systems with different compositions (wt %): (●) pure PCN; (▽) 80/20; (■) 60/40; (△) 50/50; and (—) pure PCL. The DSC traces have been shifted vertically for the sake of clarity.

a positive deviation was observed for all the PCL contents considered. Nevertheless, the variation of  $T_g$  with PCL mass fraction ( $w_{\text{PCL}}$ ) could well be fitted using the Gordon–Taylor equation [eq. (4)]<sup>20</sup> as follows:

$$T_g = \frac{[w_{\text{PCL}} \times T_{g \text{ PCL}} + k \times (1 - w_{\text{PCL}}) \times T_{g \text{ PCN}}]}{[w_{\text{PCL}} + k \times (1 - w_{\text{PCL}})]} \quad (4)$$

where  $T_{g \text{ PCN}}$  and  $T_{g \text{ PCL}}$  stand for the glass transition temperatures of pure PCN and PCL, respectively, while  $k$  is treated as a fitting parameter and is equal to 0.67. Such a  $k$  value may suggest relatively weak intermolecular interactions between both PCN and PCL components.

The width of the glass transition domains ( $\Delta T_g$ ) is approximately equal to  $(40 \pm 5)^\circ\text{C}$  (Table III). This width can be correlated to that of the relaxation time

**TABLE III**  
Glass Transition Temperatures from DSC for PCN/PCL Systems as a Function of Composition

| PCN/PCL composition (wt %) | Glass transition range ( $^\circ\text{C}$ ) |                     |              |
|----------------------------|---|---------------------|--------------|
|                            | $T_{g \text{ onset}}$                       | $T_{g \text{ end}}$ | $\Delta T_g$ |
| 100/0                      | 219   | 253                 | 34           |
| 95/5                       | 186   | 232                 | 46           |
| 90/10                      | 176   | 217                 | 41           |
| 85/15                      | 156   | 204                 | 48           |
| 80/20                      | 162   | 198                 | 36           |
| 70/30                      | 79  | 130                 | 51           |
| 60/40                      | 72  | 110                 | 38           |
| 50/50                      | 66  | 104                 | 38           |

distribution at the glass transition. The usual and convenient way to take this into account is through the stretched exponential response function for structural relaxation  $\psi(t)$  [eq. (5)]<sup>21</sup> as follows:

$$\psi(t) = \exp\left(-\left(\frac{t}{\tau}\right)^\beta\right) \quad (5)$$

where the nonexponential  $\beta$  parameter ( $0 \leq \beta \leq 1$ ) is inversely related to the width of the distribution of relaxation times.

The dependence of  $\beta$  on  $\Delta T_g$  has been demonstrated by Saiter et al.,<sup>22</sup> and according to their work, we may expect a value of  $\beta$  ranging from 0.2 to 0.4. This low value of  $\beta$  confirms the occurrence of a large distribution of relaxation times, which is usual for thermosets.

Figures 7 and 8 show, respectively, the temperature dependence of storage ( $E'$ ) and loss ( $E''$ ) moduli for the PCN matrix and different PCN/PCL systems as investigated by DMTA. Clearly, three relaxation processes could be detected in the isochronal plot obtained at 1 Hz for neat PCN: the  $\alpha$ -relaxation close to  $218^\circ\text{C}$  as well as two subglassy relaxations (the  $\beta$ - and  $\gamma$ -processes), located at  $-18^\circ\text{C}$  and close to  $-100^\circ\text{C}$ , respectively. The molecular motions underlying both  $\beta$ - and  $\gamma$ -relaxations have not been fully elucidated experimentally. Nonetheless, molecular simulations carried out on the dicyanate ester of bisphenol A (DCBA)-derivatized PCN network have suggested that the  $\gamma$ -relaxation could be attributed to rotations of the phenyl rings, while the  $\beta$ -process could be induced by rotations of the entire chain segment between triazine crosslinks.<sup>23</sup> The location of the subglassy relaxations was in agreement with the results previously reported.<sup>23</sup> As far as the PCL

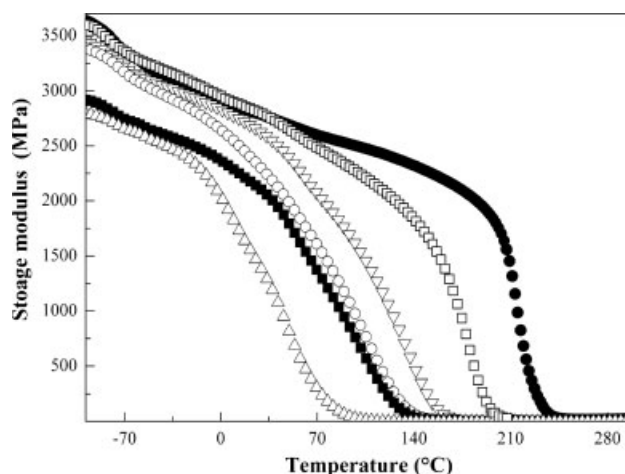


**Figure 7** Storage modulus ( $E'$ ) versus temperature for several PCN/PCL compositions (wt %): (●) pure PCN; (□) 90/10; (▽) 80/20; (○) 70/30; (■) 60/40; and (△) 50/50.

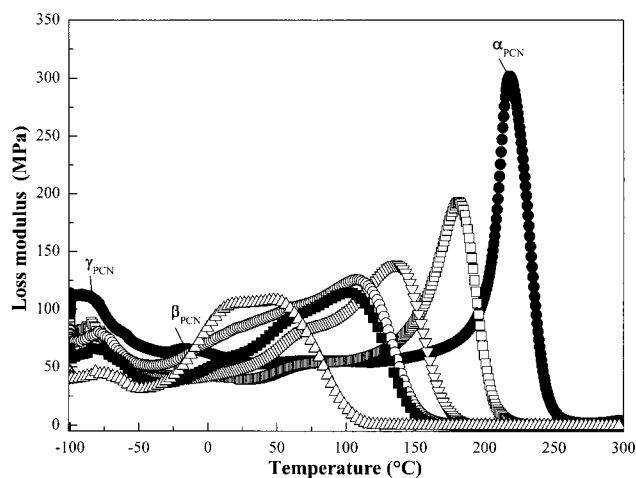


**Figure 8** Loss modulus ( $E''$ ) versus temperature for several PCN/PCL compositions (wt %): (●) pure PCN; (□) 90/10; (▽) 80/20; (○) 70/30; (■) 60/40; and (△) 50/50.

oligomer is concerned, the only thermal events that could be detected between  $-100$  and  $300^\circ\text{C}$  were the  $\alpha$ -relaxation related to the amorphous phase of semi-crystalline PCL (around  $-50^\circ\text{C}$ ) and the melting of the PCL crystallites (around  $65^\circ\text{C}$ ).

Let us consider now the changes observed on both  $E'(T)$  and  $E''(T)$  variations when increasing the PCL content up to 50 wt % in PCN/PCL systems. As can be seen in Figures 7–9, the  $\alpha$ -relaxation was strongly affected by modifying PCN with PCL oligomers. The corresponding peak displayed both a significant shift toward lower temperatures and a strong broadening, as PCL oligomers were introduced into the PCN matrix. In addition, these mechanical measurements permitted to precise the shape of the  $\alpha$ -relaxation process: the temperature dependence of  $E''$  exhibited a bimodal relaxation time distribution for this pro-

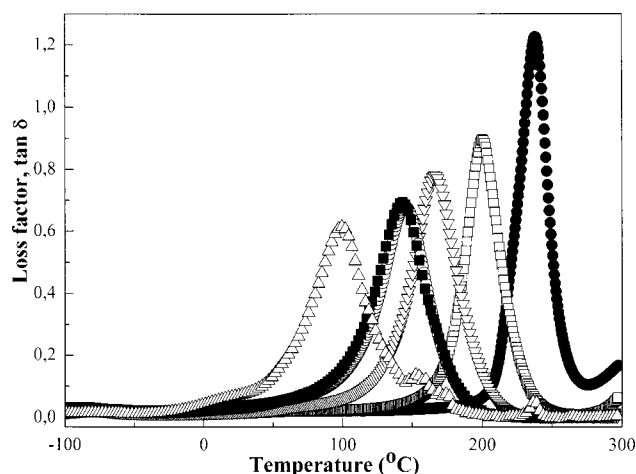


**Figure 9** Loss factor ( $\tan \delta$ ) versus temperature for several PCN/PCL compositions (wt %): (●) pure PCN; (□) 90/10; (▽) 80/20; (○) 70/30; (■) 60/40; and (△) 50/50.

cess, the bimodal shape being more and more pronounced as the PCL content was increased. This feature could be ascribed to the occurrence of two kinds of local environments within the PCN/PCL systems: a PCN-rich phase, mainly constituted of PCN crosslinked chains modified by PCL embeddings, and a PCN-PCL mixed phase formed by PCL-modified PCN network and unreacted free PCL oligomers. Moving on to the secondary relaxations related to the PCN matrix, it is observed in Figure 8 that the  $\beta$ -relaxation could hardly be detected for PCL mass fractions higher than 20 wt %, because of the strong overlapping with the  $\alpha$ -peak. Within the experimental uncertainties, the  $\gamma$ -relaxation seemed to be nearly unaffected by the incorporation of PCL oligomers: the local motions underlying this secondary relaxation (phenyl ring rotation) should not be modified in the PCN/PCL systems. Only the amplitude of this process was modulated by the PCL content, in agreement with the dilution laws, as evidenced by the linear composition dependence of the  $E''$  value measured at the  $\gamma$ -peak maximum (Fig. 10).

Finally, in a preliminary investigation, an original route to porous PCN thermosets was envisaged through the selective hydrolysis of PCL subchains from PCN/PCL networks. We adopted similar experimental conditions than those utilized elsewhere for the partial degradation of oligoester-derivatized systems.<sup>24</sup> Under the mild conditions chosen (see Experimental), it was checked that the pure PCN network was unaffected. Figure 11 represents the FTIR spectra of the PCN/PCL systems with 30 wt % of PCL, before and after hydrolysis. In the FTIR spectrum

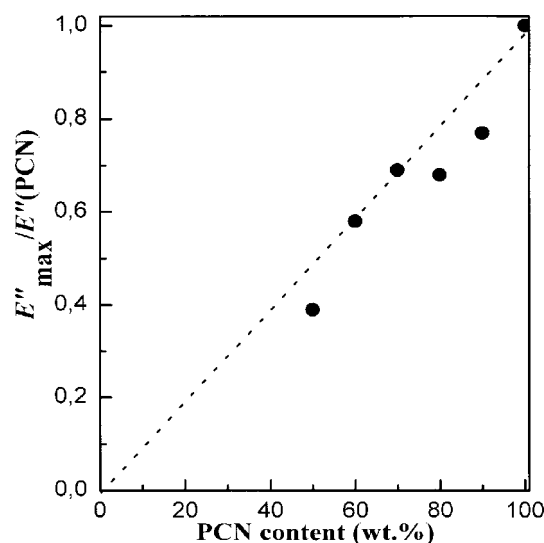


**Figure 10** Composition dependence of  $E''_{\max}/E''_{\max}(\text{PCN})$ .  $E''_{\max}$  and  $E''_{\max}(\text{PCN})$  hold for the values of the  $E''$  modulus at the maximum of the  $\gamma$ -relaxation peak observed for PCN/PCL systems and neat PCN, respectively.



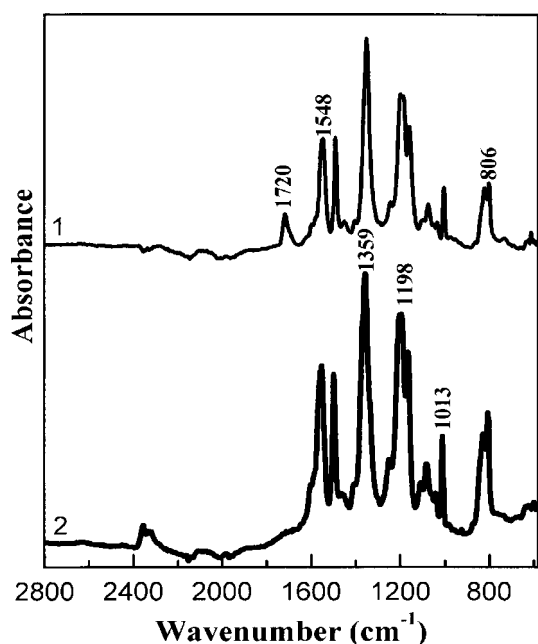


**Figure 11** FTIR spectra for PCN-containing systems with 30 wt % of PCL before (1) and after (2) hydrolysis.

of the hydrolyzed PCN/PCL hybrid network, one can clearly see the absence of the strong absorption band around  $1720\text{ cm}^{-1}$  corresponding to  $\text{C}=\text{O}$  group of the PCL component, which gives evidence of the complete hydrolysis and removal of PCL from the hybrid system. The morphologies of such PCN-based networks, before and after hydrolysis, were examined by SEM (Fig. 12). The nondegraded sample displayed a compact structure without any pore. After hydrolysis, the resulting PCN network exhibited a porous structure with pore sizes ranging from 10 to 100 nm, thus illustrating the effective role of PCL oligomer as a porogen. Obviously enough, these preliminary results only constitute a proof of concept

and deserve further investigation. Additional experiments are currently under progress.

## CONCLUSIONS

PCN networks modified by dihydroxy-telechelic oligo( $\epsilon$ -caprolactone) were synthesized via thermal polycyclotrimerization of dicyanate ester of bisphenol E in the presence of the reactive modifier. The TGA investigation of the networks with varying PCN/PCL compositions has permitted to define two groups of systems. The first group with a low content of oligo( $\epsilon$ -caprolactone) (i.e., up to 20 wt %) has been described as single phase systems. It has been shown by FTIR, gel fraction content and density measurements that the major part of the oligomeric modifier was chemically incorporated into the PCN network structure, for this group. The second group with a higher content of oligo( $\epsilon$ -caprolactone) (i.e., higher than or equal to 30 wt %) has been defined as multiphase systems, in which a significant amount of the modifier has not been covalently linked to the PCN network. Interestingly, the TGA has also showed that there is no drastic reduction in thermal stability of PCN-type networks, whatever the PCL content introduced into the structures. The DSC and DMTA study of their solid-state organization has evidenced the occurrence of at least a two-phase structure with two kinds of local environments within such PCN/PCL systems: first, a PCN-rich phase, mainly constituted of PCN crosslinked chains modified by PCL embeddings, and second, a mixed phase formed by PCL-modified PCN network and unreacted free oligo( $\epsilon$ -caprolactone).

Preliminary studies have shown that the polymer systems studied can be effectively used as precursors for the generation of porous cyanurate thermosetting materials through the quantitative hydrolysis of the

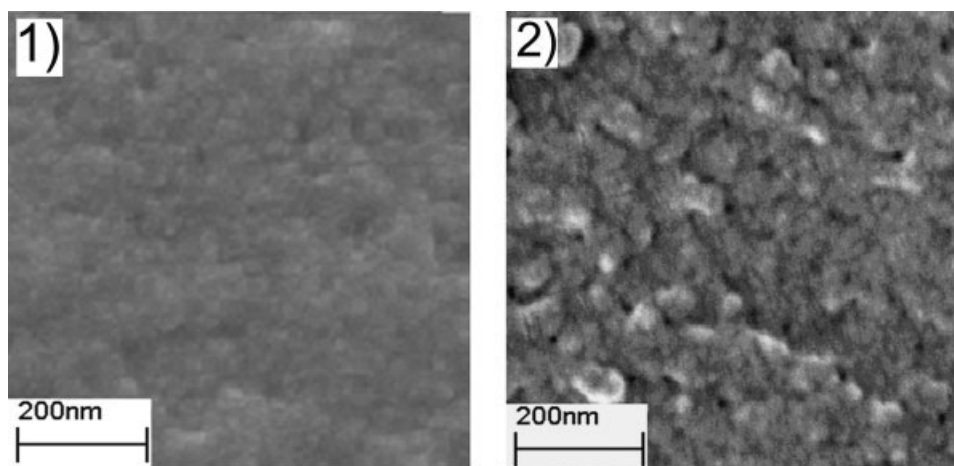


**Figure 12** SEM micrographs of PCN/PCL systems (70/30 wt %) before (1) and after (2) hydrolysis.

oligo( $\epsilon$ -caprolactone) subchains. Further investigation with a thorough characterization of porous materials is under progress and will be published in a forthcoming paper.

The authors thank Mrs. I. Danylenko, K. Gusakova, O. Starostenko, and N. Lacoudre for their kind technical assistance.

## References

1. Hamerton, I., Ed. *Chemistry and Technology of Cyanate Ester Resins*; Chapman & Hall: Glasgow, 1994.
2. Fainleib, A. M.; Shantalii, T. A.; Pankratov, V. A. *Compos Polym Mater (Kiev)* 1991, 49, 39.
3. Fainleib, A. M.; Sergeeva, L. M.; Shantalii, T. A. *Compos Polym Mater (Kiev)* 1991, 50, 63.
4. Hamerton, I.; Hay, J. N. *High Perform Polym* 1998, 10, 163.
5. Nair, C. P. R.; Mathew, D.; Ninan, K. N. *Adv Polym Sci* 2000, 155, 1.
6. Grigoryeva, O.; Fainleib, A.; Sergeeva, L. M. In *Handbook of Condensation Thermoplastic Elastomers*; Fakirov, S., Ed.; Wiley-VCH: Weinheim, 2005; Chapter 12, pp 325–354.
7. Fainleib, A.; Grigoryeva, O.; Pissis, P. *J Balkan Tribolog Assoc* 2005, 11, 303.
8. Fainleib, A.; Grigoryeva, O.; Hourston, D. *Macromol Symp* 2001, 164, 429.
9. Fainleib, A.; Hourston, D.; Grigoryeva, O.; Shantalii, T.; Sergeeva, L. *Polymer* 2001, 42, 8361.
10. Fainleib, A. M.; Grigoryeva, O. P.; Hourston, D. J. *Int J Polym Mat* 2001, 51, 57.
11. Fainleib, A.; Grenet, J.; Garda, M. R.; Saiter, J. M.; Grigoryeva, O.; Grytsenko, V.; Popescu, N.; Enescu, M. C. *Polym Degrad Stab* 2003, 81, 423.
12. Kiefer, J.; Hilborn, J. G.; Hedrick, J. L.; Cha, H. J.; Yoon, D. Y.; Hedrick, J. C. *Macromolecules* 1996, 29, 8546.
13. Kiefer, J.; Porouchani, R.; Mendels, D.; Ferrer, J. B.; Fond, C.; Hedrick, J. L.; Kausch, H. H.; Hilborn, J. G. *Micropor Macropor Mater* 1996, 431, 527.
14. Hedrick, J. L.; Russell, T. P.; Hedrick, J. C.; Hilborn, J. G. *J Polym Sci, Part A: Polym Chem* 1996, 34, 2879.
15. Bauer, J.; Bauer, M. In *Chemistry and Technology of Cyanate Ester Resins*; Hamerton, I., Ed.; Chapman & Hall: Glasgow, 1994. pp 58–86.
16. Elzein, T.; Nasser-Eddine, M.; Delaite, C.; Bistac, S.; Dumas, P. *J Colloid Interface Sci* 2004, 273, 381.
17. Colthup, N. B.; Daly, L. H.; Wiberley, S. E., Eds. *Introduction to Infrared and Raman Spectroscopy*; Academic Press: San Diego, 1990; pp 227–231.
18. Grigat, E.; Putter, R. *Angew Chem Int Ed* 1967, 6, 206.
19. Jho, J. Y.; Yee, A. F. *Macromolecules* 1991, 24, 1905.
20. Gordon, M.; Taylor, J. S. *J Appl Chem* 1952, 2, 493.
21. Williams, G.; Watts, D. C. *Trans Faraday Soc* 1970, 66, 80.
22. Saiter, A.; Devallencourt, C.; Saiter, J. M.; Grenet, J. *Eur Polym Mater* 2001; 37: 1083.
23. Georjon, O.; Schwach, G.; Gérard, J. F.; Galy, J.; Albrand, M.; Dolmazon, R. *Polym Eng Sci* 1997, 37, 1606.
24. Grande, D.; Renard, E.; Langlois, V.; Rohman, G.; Timbart, L.; Guérin, Ph. In *Degradable Polymers and Materials—Principles and Practice*; Khemani, K.; Scholz, C., Eds. *American Chem Society*, 2006; Chapter 9, pp 140–155. ACS Symposium Series 939.